

# Silencing of WWP2 inhibits adhesion, invasion, and migration in liver cancer cells

Yong Qin<sup>1</sup> · Sheng-qian Xu<sup>1</sup> · De-biao Pan<sup>1</sup> · Guan-xiong Ye<sup>1</sup> · Cheng-jun Wu<sup>1</sup> · Shi Wang<sup>1</sup> · Chao-jun Wang<sup>1</sup> · Jin-yan Jiang<sup>1</sup> · Jing Fu<sup>1</sup>

Received: 7 September 2015 / Accepted: 30 November 2015 / Published online: 10 December 2015  
© International Society of Oncology and BioMarkers (ISOBM) 2015

**Abstract** The role and clinical implication of the WWP2 E3 ubiquitin ligase in liver cancer are poorly understood. In the current study, we investigated the expression level of WWP2 and its functions in cell adhesion, invasion, and migration in liver cancer. We used real-time PCR to detect the expression of WWP2 in liver cancer and adjacent samples from the People's Hospital of Lishui and also analyzed The Cancer Genome Atlas (TCGA) RNA-seq data by bioinformatics. Migration and invasion were detected by transwell analysis. We detected a strong WWP2 expression in tumor tissues of the People's Hospital of Lishui, and the survival rate was significantly higher in patients with lower WWP2-expressing tumors. WWP2 small hairpin RNA (shRNA) lentivirus stably infected cells (shWWP2), Huh7, showed slower growth speed compared with scramble control-infected cells in a xenograft mouse model. Knockdown of WWP2 Huh7 and BEL-7404 cells demonstrated a reduction in adhesion, invasion, and migration. Gene set enrichment analysis (GSEA) showed that WWP2 is positively correlated to cancer-related pathways including the chemokine signaling pathway. WWP2 also regulated MMP-9, caspase-9, CXCR3, and CCR5 expression in liver cancer cells. In addition, knockdown of CXCR3 and CCR5 significantly inhibited cell proliferation, adhesion, invasion, and migration in Huh7

and BEL-7404 cells. Our data suggest that targeting of WWP2 may be a therapeutic strategy for liver cancer treatment.

**Keywords** Liver cancer · WWP2 · Carcinogenesis · Chemokine signaling pathway

## Introduction

As the third leading cause of death from cancer, hepatocellular carcinoma (HCC) accounts for the great proportion in primary liver cancers and ranks as the fifth most common malignancy all over the world [1]. In the earlier stages of HCC, curative resection and partial ablation therapy are often applied to patients [2, 3]. However, because of the high recurrence and metastasis rates after surgery and ablation therapy, HCC patients are often accompanied with poor prognosis [4]. Therefore, inhibiting metastasis of HCC patients is critical for HCC therapy.

Genes and proteins associated with the development and progression of HCC were investigated in preceding studies [5, 6]. Recently, an E3 ubiquitin ligase that belongs to the NEDD4-like protein family termed WWP2 was implicated in HCC progression [7]. WWP2 is a member of the NEDD4 subfamily originally identified in screening for WW domain-containing proteins [8]. So far, a very limited number of substrates have been reported for WWP2, such as Oct4, PTEN, Rpb1, EGR-2, Gsc, Sox9, and the epithelial Na<sup>+</sup> channel [9–11]. There are a variety of data focusing on the novel tumorigenesis effects of WWP2 [12, 13]. Meanwhile, gene silencing studies have revealed a significant role of WWP2 in craniofacial development [14] and chondrogenesis [15].

Cancer pathway especially chemokine signaling pathway contributes to the development and progression of cancer, in which they function in several capacities [16–18]. Matrix

**Electronic supplementary material** The online version of this article (doi:10.1007/s13277-015-4547-z) contains supplementary material, which is available to authorized users.

✉ Sheng-qian Xu  
xushengqian162@163.com

<sup>1</sup> Department of Hepatobiliary Surgery, People's Hospital of Lishui, 15 Public Street, Liandu District, Lishui 323000, China

metalloproteinase 9 (MMP-9) was reported to induce cell invasion and migration in various cancers via p38 MAPK, ERK, AKT, JNK, and PKC signaling pathways [19, 20]. Caspase-9 plays a critical role in tumorigenesis through mediating oncogene and apoptosis [21]. Chemokine receptors, CXCR3 and CCR5, have opposing effects on inflammation in the central nervous system of virus-infected mice [22]. But the possible contribution of chemokine receptor signaling to the guidance of cell invasion and migration has not been explored.

In this study, our data reveal a new insight into WWP2-mediated regulation of chemokine signaling that permits further investigation of WWP2 as a novel cancer prognostic marker and therapeutic target.

## Materials and methods

### Ethics statement

The study protocol was approved by the ethics committee of the People's Hospital of Lishui. Written informed consents were obtained from all participants in this study. All the research was carried out in accordance with the Helsinki Declaration of 1975. Care of laboratory animals and animal experimentation were performed in accordance with the Guide for the Care and Use of Laboratory Animals of the National Institutes of Health. All animal studies were approved by the animal ethics committee of the People's Hospital of Lishui.

### Patients and tissue sample preparations

Paired tumor and adjacent human liver samples were obtained from 47 patients who underwent surgery at the People's Hospital of Lishui. None of these patients had received radiotherapy or chemotherapy. The percentage of tumor cellularity in the liver cancer patient's tissue section is at least 70 % via pathological examination of histology slides in hospital patient's cohort. Liver cancer and adjacent tissues were immediately snap-frozen in liquid nitrogen and stored at  $-80^{\circ}\text{C}$  until total RNA was extracted. The clinical information of 47 liver cancer patients is listed in Supplemental Table 1.

### Bioinformatics analysis

RNA-Seq data from 191 liver cancers and 50 adjacent tissues was downloaded from The Cancer Genome Atlas (TCGA) and survival rate data was downloaded from the NCBI Gene Expression Omnibus (GEO, <http://www.ncbi.nlm.nih.gov/geo/>) and is accessible through GEO Series accession number GSE20140, following approval of this project by the consortium. To validate the correlation of WWP2 and pathways in cancer especially the chemokine signaling

pathway involved in the pathogenesis of liver cancer, a gene set enrichment analysis (GSEA) was performed to analyze the liver cancer tumors in KEGG dataset. GSEA is a method of analyzing and interpreting microarray and such data using biological knowledge [23]. If a gene set has a positive enrichment score, the majority of its members have higher expression accompanied with higher WWP2 expression, and the set was termed "enrich" [24].

### Immunohistochemistry

Initial treatments for tissue sections were deparaffinization and hydration and then they were heated in EDTA (pH 8.0) and incubated with 3 % hydrogen peroxide for 10 min for antigen retrieval. The reaction of WWP2 antibody (Abcam) took place for 1 h at room temperature, following incubation with biotin-labeled secondary antibodies. Slides were stained with DAB (Shanghai Long Island Biotech. Co., Ltd., China) and hematoxylin (BASO, China). Immunohistochemical signals were calculated with the positive staining cells under a microscope (Olympus Corporation, Tokyo, Japan) with a magnification of  $\times 200$ .

### Cell culture and construction of stable cell lines

Seven liver cancer cell lines (MHCC97H, LM3, SMCC7721, HepG2, Hep3B, Huh7, BEL-7404) obtained from the Cell Bank of Academia Sinica (Shanghai, China) were used in this study. The cells were cultured in Dulbecco's modified Eagle's medium (DMEM) with 10 % fetal bovine serum (FBS) in a humidified incubator containing 5 %  $\text{CO}_2$  in air at  $37^{\circ}\text{C}$ . Commercial WWP2, CXCR3, and CCR5 small hairpin RNA (shRNA)-expressing vectors were obtained from JRDUN Biotechnology (Shanghai, China). The shRNA sequences were cloned into the pLVX-AcGFP-C1 lentiviral vector. The scramble shRNA was cloned into the pLVX-AcGFP-C1 lentiviral vector and used as a negative control (shNC). The constructs were then co-transfected into HEK 293T cells with lentiviral packaging vectors by using Lipofectamine 2000 (Invitrogen Life Technologies, Gaithersburg, MD, USA) according to the manufacturer's instruction. Then the lentivirus packaging, purification, concentration, and infection were performed as described by Xiong et al. [25]. Viruses were collected 48 h after transfection and used to infect Huh7 and BEL-7404 cells at an MOI of 20 in the presence of 8  $\mu\text{g/ml}$  Polybrene (Sigma-Aldrich, St. Louis, MO, USA). Assay was performed 48 h after infection.

### Quantitative real-time PCR

Total RNAs were extracted from 47 paired adjacent and human liver cancer tissues and seven liver cancer cells with TRIzol reagent (Invitrogen) as described [26] and stored at

–80 °C. Complementary DNA was synthesized with a complementary DNA synthesis kit (Thermo Fisher Scientific, Rockford, IL, USA). Real-time PCR was performed on ABI 7500 (Applied Biosystem, Foster City, CA, USA) thermal cycler using a standard SYBR Green PCR kit (Thermo Fisher Scientific). Real-time PCR was performed to detect messenger RNA (mRNA) levels of indicated genes. The primers sequences (sense/antisense) used were listed as follows: WWP2, 5'-GAGATGGACAACGAGAAG-3' and 5'-CTCCTCAATGGCATAACAG-3'; GAPDH, 5'-CACCCACTCCTCCACCTTTG-3' and 5'-CCACCACCCTGTTGCTGTAG-3'. Relative quantification of the gene expression was performed by normalization of the signals of different genes with the GAPDH signal. Each experiment was performed in triplicate.

### In vitro proliferation assay

Cell proliferation was assessed by Cell Counting Kit 8 (CCK-8; Dojindo, Kumamoto, Japan) assay. In brief, we plated the cells in 96-well plates at an initial density of  $5 \times 10^3$  cells/well. Cells were subsequently infected with pLVX-AcGFP-C1-WWP2 shRNA (shWWP2), pLVX-AcGFP-C1-CXCR3 shRNA (shCXCR3), or pLVX-AcGFP-C1-CCR5 shRNA (shCCR5) following culture overnight. At specified time points, 10  $\mu$ l of CCK-8 solution was added to each well of the plate. Then the plate was incubated for 1 h. Cell proliferation was determined by scanning with a microplate reader (Bio-Rad Laboratories, Hercules, CA, USA) at 450 nm. Each experiment was performed in triplicate.

### In vitro apoptosis assay

Apoptosis was determined by a flow cytometer (BD Biosciences, San Diego, CA, USA), and annexin-V fluorescein isothiocyanate (FITC)/propidium iodide (PI) double-stain assay was performed in accordance with the manufacturer's protocol (BioVision, Mountain View, CA, USA). Briefly, cells were seeded into six-well plates, infected with the shWWP2, and cultured for 48 h. The cells were subsequently collected and incubated with FITC and PI, prior to analysis by flow cytometry. Each experiment was performed in triplicate.

### In vitro adhesion assay

Cells treated with shWWP2, shCXCR3, or shCCR5 were seeded on fibronectin-coated 12-plate microplate at a density of  $1 \times 10^5$  cells/well and then incubated for 1 h. The supernatant was discarded and cells were washed two times by phosphate-buffered saline (PBS, Gibco). Four percent paraformaldehyde (Gibco) was supplemented for 15 min and cells were stained by Giemsa (Gibco) for 30 min. Images of the

cells were captured and cell numbers were counted under a microscope (Olympus Corporation) with magnification of  $\times 400$ . Each experiment was performed in triplicate.

### In vitro invasion assay

Invasion assays were performed using transwell chamber (Greiner Bio-One, Frickenhausen, Germany) coated with Matrigel (BD, San Diego, CA, USA) as described in the manufacturer's protocol. Cells treated with shWWP2, shCXCR3, or shCCR5 were serum-starved for 12 h and then resuspended in DMEM.  $1 \times 10^5$  cells in 500  $\mu$ l serum-free DMEM were seeded into the upper well of the transwell chamber. The lower chamber was filled with 600  $\mu$ l DMEM containing 10 % FBS. After 48-h incubation, cells on the upper well were wiped off by the Q-tip. The cells attached to the lower surface were washed with PBS, fixed in 4 % paraformaldehyde, and stained by 0.5 % crystal violet. Images of the cells were captured and cell numbers were counted under a microscope (Olympus Corporation) with magnification of  $\times 400$ . Each experiment was performed in triplicate.

### In vitro migration assay

Cell transwell migration assays were performed according to the previous study [27]. Briefly, cells treated with shWWP2, shCXCR3, or shCCR5 were trypsinized, washed, and kept suspended in DMEM. DMEM with 10 % FBS was added to the lower wells of the transwell chambers and serum-free DMEM with  $5 \times 10^4$  cells/well was filled in the upper wells of the transwell chambers. Then, the chamber was placed in an incubator at 37 °C for 24 h. Filters were fixed with 4 % methanol and stained with 0.5 % methylrosanilinium chloride solution for 30 min. Then cells on the upper well were wiped off by the Q-tip. Images of the cells were captured and cell numbers were counted under a microscope (Olympus Corporation) with a magnification of  $\times 400$ . Each experiment was performed in triplicate.

### Western blot analysis

Total proteins were isolated from normal and liver tumor tissues or liver cancer cell lines. Protein concentration was measured by BCA protein assay kit (Pierce, Rockford, IL, USA). Equal amounts of cell lysates were subjected to electrophoresis using SDS-PAGE. Then, Western blot analysis was performed. Membranes were first incubated with antibody against WWP2 (cat. no. ab103527), CXCR3 (cat. no. ab71864), CCR5 (cat. no. ab65850), MMP-9 (cat. no. ab119906), and caspase-9 (cat. no. ab2324), then with anti-GAPDH antibody as an internal control. Antibodies used in this study were purchased from Abcam (Cambridge, MA, USA), unless otherwise specified: GAPDH (CST Biotech,

Danvers, MA, USA; cat. no. 5174). All the antibodies were used at a dilution of 1:1000.

### In vivo experiments

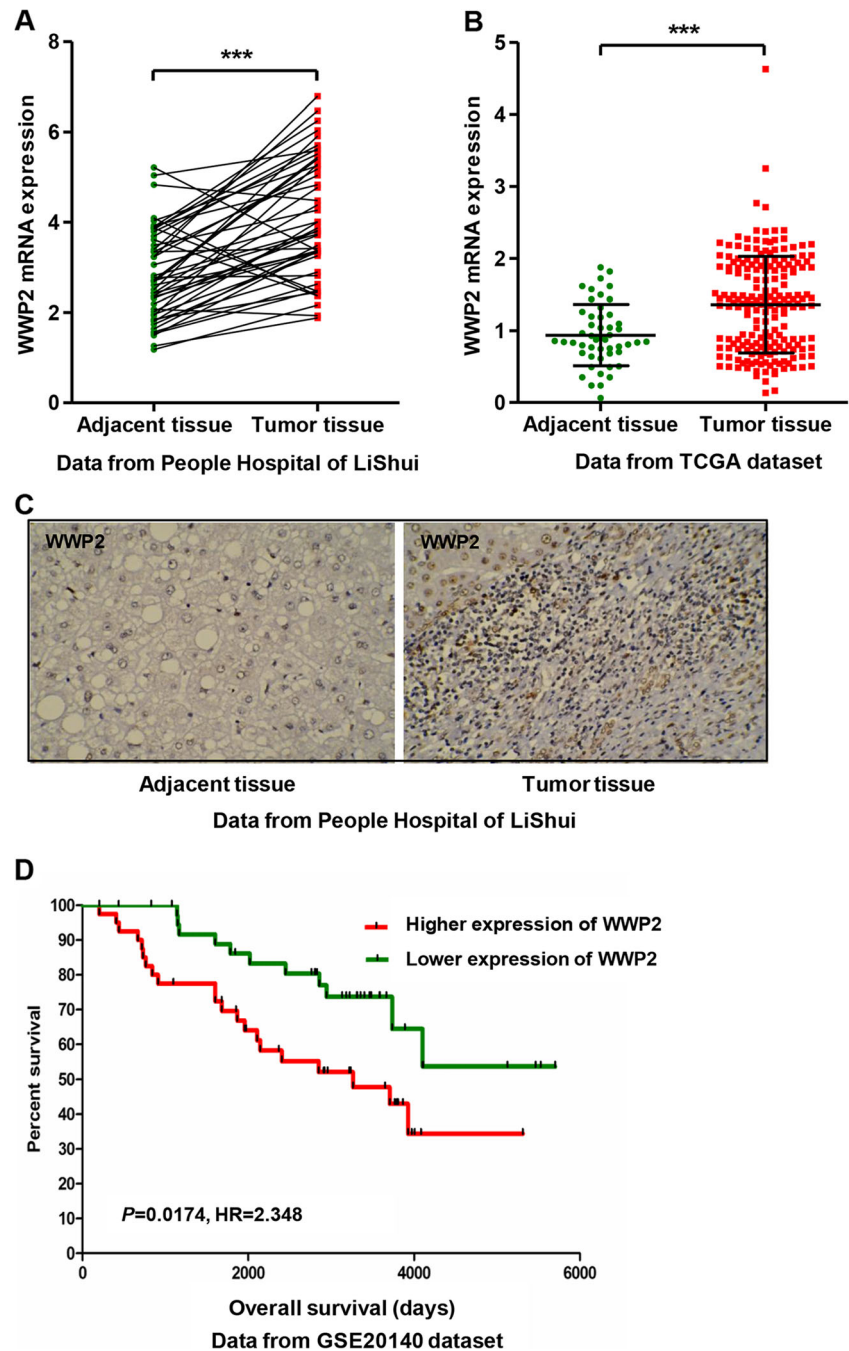
In order to clarify the role of WWP2 in vivo, 4-week-old male athymic nude mice were used in this study. Twelve male athymic nude mice were randomly divided into two groups (six mice/group). Huh7 cells ( $2 \times 10^6$ ) with negative control (shNC) or shWWP2 were injected subcutaneously into the

right flank of these mice to establish the liver cancer xenograft model. The tumor size was determined every 3–4 days after tumor formed (around 1–2 weeks) as previously described [28]. The mice were sacrificed and photographed after 45 days, and the tumors were weighed on a digital balance.

### Statistical analysis

The data was presented as the mean value  $\pm$  SD. Statistical significance was determined by the paired, two-tailed

**Fig. 1** WWP2 upregulated in liver cancer tissues and correlated with poor survival time. **a** Comparison of the expression level of WWP2 between liver cancer and adjacent tissues in the People's Hospital of Lishui by real-time PCR. **b** Bioinformatics was also used to analyze the expression level of WWP2 in TCGA RNA-seq data. **c** The expression of WWP2 was determined by immunohistochemistry staining in human liver cancer tissues. **d** Kaplan–Meier survival curves for two groups of patients. *Green*, data for patients with low prognostic scores (group 1, higher survival time); *red*, patients with high prognostic scores (group 2, poorer survival). Means  $\pm$  SD are shown. \*\*\* $P < 0.001$



Student's *t* test and one-way ANOVA analysis. Overall survival in relation to WWP2 expression was evaluated by the Kaplan–Meier survival curve and log-rank nonparametric test. *P* value lower than 0.01 was considered to be statistically significant.

## Results

### Upregulation of WWP2 expression correlates with liver cancer patient survival

Real-time PCR showed that WWP2 was significantly increased in liver cancer tissues when compared with the adjacent liver tissues of patients in the People's Hospital of Lishui, and bioinformatics analysis in TCGA RNA-seq data also demonstrated the similar results of the People's Hospital of Lishui (Fig. 1a, b). To assess the protein levels of WWP2 in human liver cancer tissues, immunohistochemistry staining of

WWP2 was performed. A high expression of WWP2 was observed in human liver cancer tissues compared with adjacent liver tissues (Fig. 1c).

Next, we compared the survival time of patients from GSE20140 dataset. The human liver cancer patients were divided into two groups according to the mean level of WWP2 (1.17 of the log<sub>2</sub> value, median in GSE20140 dataset). The cumulative survival rate was significantly higher in patients with lower WWP2-expressing tumors than in those with higher WWP2-expressing tumors (Fig. 1c). These results indicate that WWP2 expression could represent a new prognostic factor in liver cancer patients and therefore we chose to focus our experimental research on WWP2.

### Silencing of WWP2 in liver cancer cell lines

We compared gene expression of WWP2 in seven liver cancer cell lines, including MHCC97H, Huh7, BEL-7404, SMCC7721, LM3, HepG2, and Hep3B at both

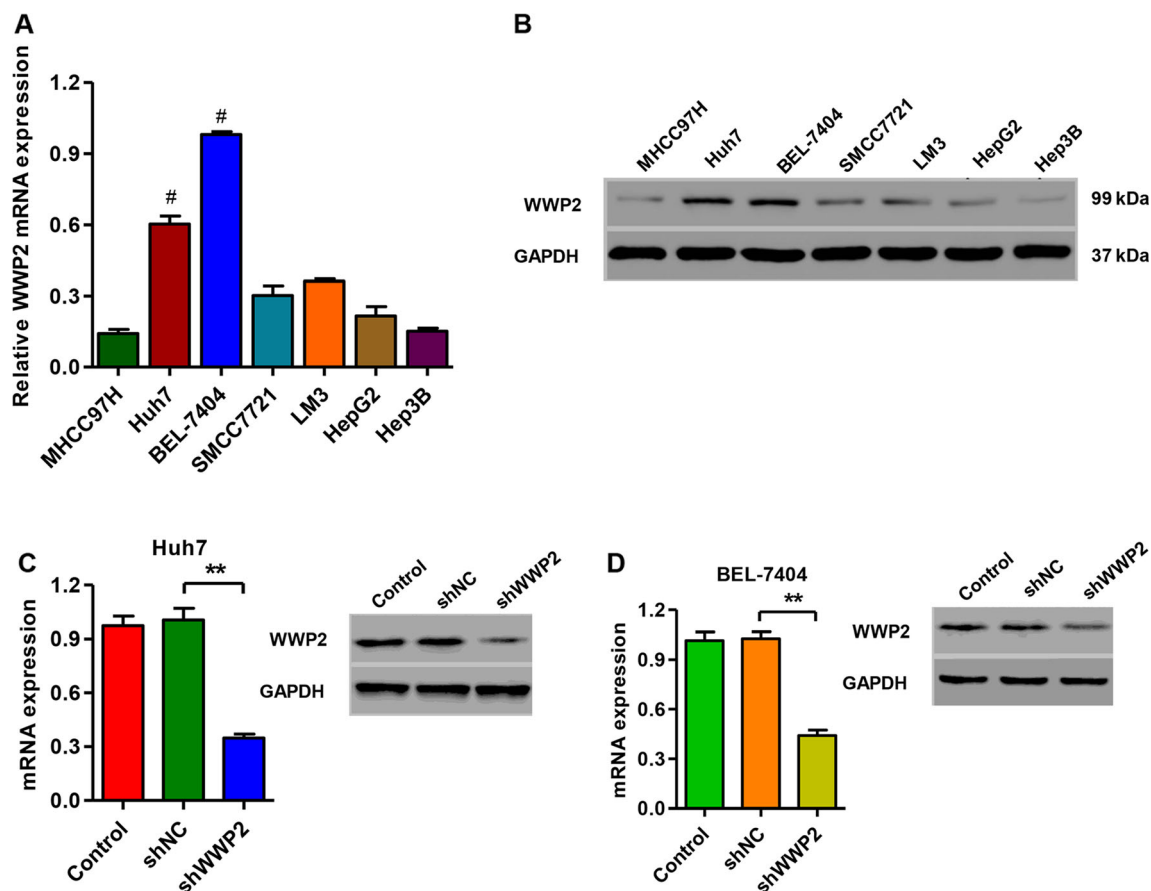


**Fig. 2** WWP2 expression in liver cancer cell lines. Cells were grown to confluence in 96-well plates. Total RNA was extracted from various liver cancer cell lines. **a** mRNA expression of WWP2 and GAPDH were determined by real-time PCR using a WWP2 specific primer set. **b** WWP2 protein expression was analyzed by Western blot using anti-WWP2 antibody. After treatment of Huh7 (**c**) and BEL-7404 (**d**) cells

with shWWP2, the expression of WWP2 assay was analyzed by real-time PCR and Western blot, as described in “Materials and methods.” Shown are representative blots of three independent studies. Means±SD are shown. #*P*<0.01 compared with five other liver cancer cell lines. \*\**P*<0.01 compared with the shNC groups

mRNA and protein levels. We found that Huh7 and BEL-7404 cells had a higher level of WWP2 expression compared with another five cells (Fig. 2a, b). These two cell lines were therefore used for subsequent experiments. mRNA and protein expression of WWP2 in response to specific shRNA was assessed. As illustrated in Fig. 2c, d, the reduction of WWP2 mRNA expression was detected after injection of shWWP2 in Huh7 ( $65 \pm 3.7\%$ ) and BEL-7404 ( $57 \pm 4.8\%$ ) cells. And the reduction of WWP2 protein expression was consistent with that of WWP2 mRNA expression in Huh7 and BEL-7404 cells. No apparent changes of negative control (NC) were observed.

### Silencing of WWP2 promotes proliferation and inhibits apoptosis in Huh7 and BEL-7404 cells

In order to further investigate the correlation between WWP2 expression and the development and progression of liver cancer, a series of in vitro and in vivo experiments was performed in Huh7 and BEL-7404 cells. The reduction of WWP2 expression led to a  $41 \pm 2.4$  and  $42 \pm 2.8\%$  proliferation decrease in Huh7 and BEL-7404 cells, respectively, at 72 h after injection compared with cells with shNC injection (Fig. 3a, b). In addition, the apoptotic rate was also detected in Huh7 and BEL-7404 cells. As shown in Fig. 3c, d, the apoptotic rate of cells injected with shWWP2 was significantly increased by  $3.1 \pm$

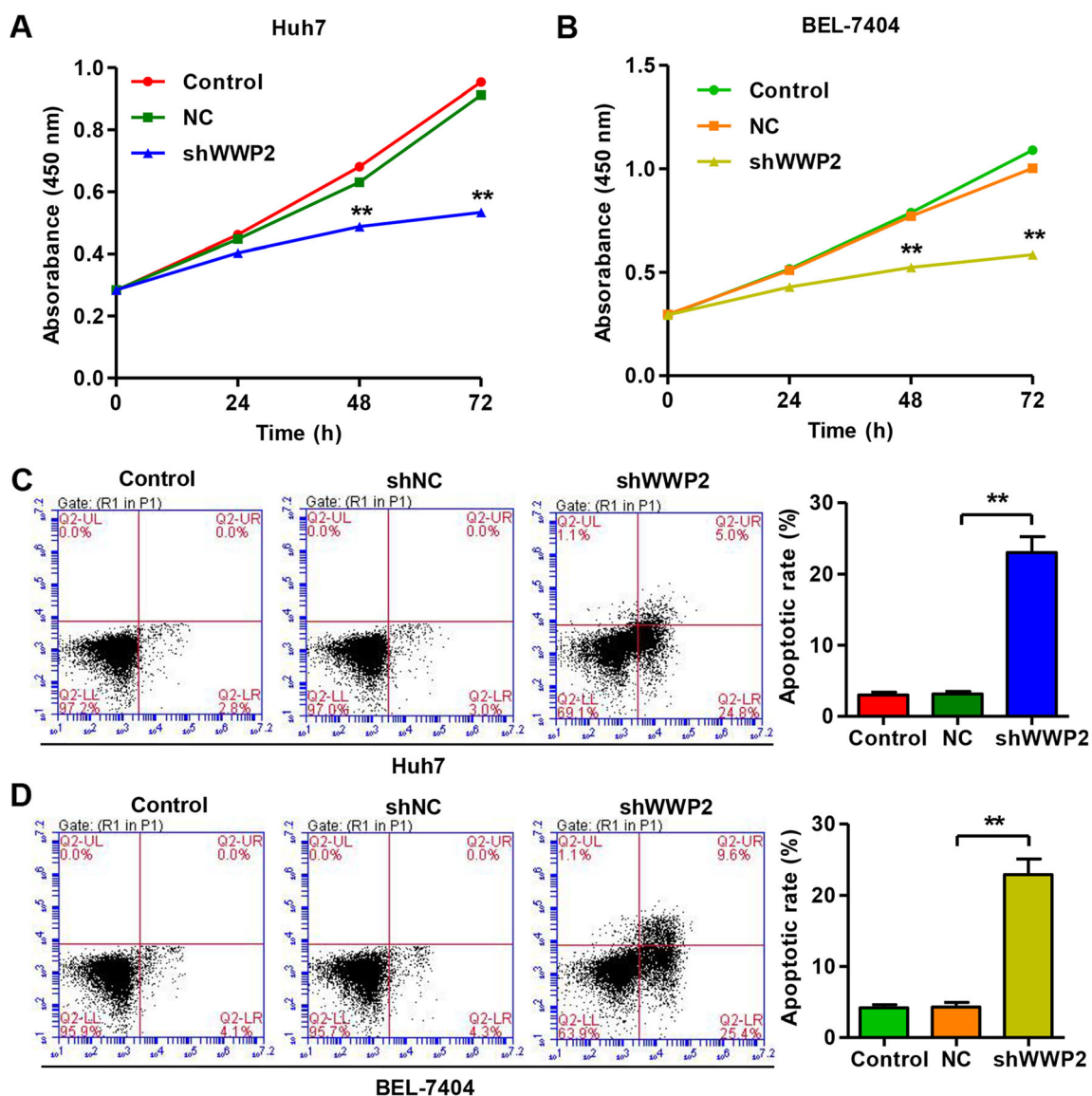


**Fig. 3** Effect of shWWP2 on cell proliferation and apoptosis. After treatment of Huh7 and BEL-7404 cells with shWWP2, cell proliferation (a) and apoptosis (b, c) were performed, as described in “Materials and

methods.” Shown are representative pictures of three independent studies. Means $\pm$ SD are shown. \*\* $P < 0.01$  compared with the shNC group

0.36 to  $23 \pm 2.21$  % (Huh7 cells) and  $4.3 \pm 0.65$  to  $23 \pm 2.16$  % (BEL-7404 cells), respectively, compared with cells with shNC injection.

### Silencing of WWP2 inhibits adhesion, invasion, and migration in Huh7 and BEL-7404 cells

Carcinoma cell adhesion to extracellular matrix and basement membranes is regarded as an initial step in the invasive process for metastatic tumor cells [29, 30]. The effects of WWP2 shRNA on liver cancer cell adhesion were identified by the cell adherence as previously described. As shown in Fig. 4a, shWWP2 could notably suppress adhesion of Huh7 ( $57 \pm 1.7$  %) and BEL-7404 cells ( $60 \pm 2.5$  %) in comparison with the negative control (shNC). As illustrated in Fig. 4b, shWWP2 but not shNC effectively suppressed cell invasion in Huh7 and BEL-7404 cells. After injection with shWWP2, the number of Huh7 and BEL-7404 cells that invaded through the filter decreased to  $33 \pm 2.4$  and  $45 \pm 3.6$  %, respectively, when compared with cells injected with shNC. According to the cell migration assay, we observed that cell migration was significantly suppressed in Huh7 ( $34 \pm 2.1$  %) and BEL-7404 cells ( $41 \pm 1.1$  %) injected with shWWP2 than in those injected with shNC (Fig. 4c). These results indicate that WWP2 is a critical mediator involved in cell invasion, migration, and adhesion.

### WWP2 is positively correlated to chemokine signaling pathway

The exact pathways that WWP2 may regulate in liver cancer remain unclear. In order to probe the WWP2-associated pathways in liver cancer tissues and cells, we first performed GSEA using high throughput RNA-sequencing data of the liver cancer tumors of KEGG database. GSEA is used to detect coordinated differences in the expression of predefined KEGG sets of functionally related genes [24]. Among all the predefined KEGG gene sets, the cancer pathway especially the chemokine signaling pathway was identified with the strongest association with WWP2 expression (Fig. 5a, b), and the gene alternations in these signaling pathways are listed in Supplemental Tables 2 and 3.

To validate the results in Western blot, we performed Western blot analysis in liver cancer cells. The gene expression of important regulators in cancer pathways was determined in protein levels in Huh7 and BEL-7404 cells. The protein level of MMP-9 ( $47 \pm 2.9$  % reduction of Huh7 cells;  $77 \pm 3.2$  % reduction of BEL-7404 cells) was remarkably decreased after downregulation of WWP2, but the protein level of caspase-9 ( $>2.0$ -fold increase of Huh7 cells;  $>1.5$ -fold increase of BEL-7404 cells) was remarkably increased after downregulation of WWP2 (Fig. 5c). The gene expression of important regulators in chemokine signaling pathway was also determined in protein levels in Huh7 and BEL-7404 cells. The

protein levels of CXCR3 ( $74 \pm 2.4$  % reduction of Huh7 cells;  $84 \pm 3.7$  % reduction of BEL-7404 cells) and CCR5 ( $70 \pm 2.2$  % reduction of Huh7 cells;  $64 \pm 1.8$  % reduction of BEL-7404 cells) were remarkably decreased after downregulation of WWP2 (Fig. 5d).

### Silencing of CXCR3 and CCR5 inhibits proliferation and motility in Huh7 and BEL-7404 cells

As CXCR3 and CCR5 expression levels related to WWP2-mediated chemokine signaling pathway in liver cancer, we wonder whether CXCR3 and CCR5 might associate with the development and progression of liver cancer. We thus performed proliferation assay by CCK-8 in Huh7 and BEL-7404 cells. As illustrated in Fig. 6a, b, silencing of CXCR3 and CCR5 through injection of shCXCR3 or shCCR5 into Huh7 and BEL-7404 cells resulted in the reduction of CXCR3 and CCR5 protein expression. Silencing of CXCR3 and CCR5 in Huh7 and BEL-7404 cells significantly decreased cell proliferation by nearly twofold at 72 h compared with cells injected with shNC (Fig. 6c–f). These results showed that CXCR3 and CCR5 had proliferation-promoting properties in liver cancer cells.

Next, we further investigate the effects of CXCR3 and CCR5 on adhesion, invasion, and migration in Huh7 and BEL-7404 cells. As shown in Fig. 7a, b, injection of shCXCR3 or shCCR5 into Huh7 and BEL-7404 cells significantly reduced the cell adhesion ability compared with cells injected with shNC. The similar functions of CXCR3 and CCR5 on invasion and migration were also detected in Huh7 and BEL-7404 cells (Fig. 7c–f). These data suggested that CXCR3 and CCR5 promoted liver cancer cell adhesion, invasion, and migration.

### Silencing of WWP2 suppresses tumor growth of liver cancer cells in vivo

Next, we determined whether silencing of WWP2 could reduce liver cancer cell growth in vivo. Huh7 cells injected with shNC and shWWP2 were subcutaneously injected in athymic nude mice respectively and tumor diameter was evaluated for 45 days. As shown in Fig. 8a, tumor diameter was significantly decreased in mice with injection of shWWP2 stably infected cells compared with control group. As shown in Fig. 8b, WWP2 silenced tumors grew slower in mice, whereas control tumors grew fast in mice. After 45 days, tumor weights in shWWP2-treated mice were significantly decreased to  $18 \pm 1.2$  % compared with the control group (Fig. 8c). These results indicate that decrease of WWP2 reduces tumor growth in vivo.

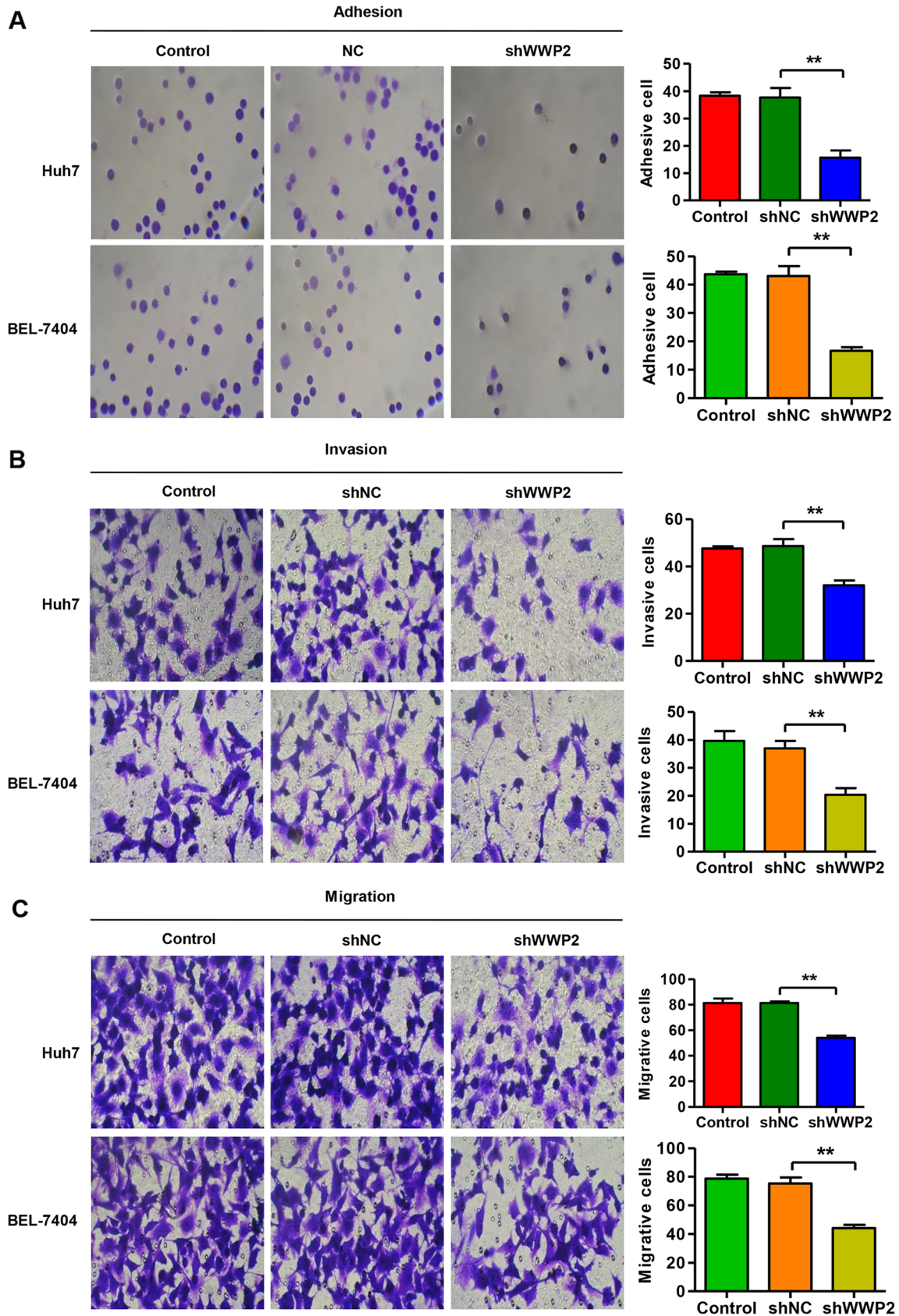




**Fig. 4** Effect of shWWP2 on cell adhesion, invasion, and migration. After treatment of Huh7 and BEL-7404 cells with shWWP2, cell adhesion (a), invasion (b), and migration (c) were performed, as described in “Materials and methods.” Shown are representative pictures of three independent studies. Means±SD are shown. \*\**P*<0.01 compared with the shNC group

expression and underlying role of WWP2 in liver cancer is largely lacking. The current study showed that mRNA expression of WWP2 was significantly increased in liver tumor tissues and Huh7 and BEL-7404 liver cancer cell lines compared with normal tissues and other liver cancer cell lines. The survival rate was higher in patients with lower WWP2-expressing tumors than in those with higher WWP2-expressing tumors. Downregulation of WWP2 in liver cancer inhibits cell adhesion, invasion, and migration in vitro and tumor formation in vivo.

**Discussion**

In recent years, although WWP2 has been broadly studied in different cancers, the knowledge of the abnormal

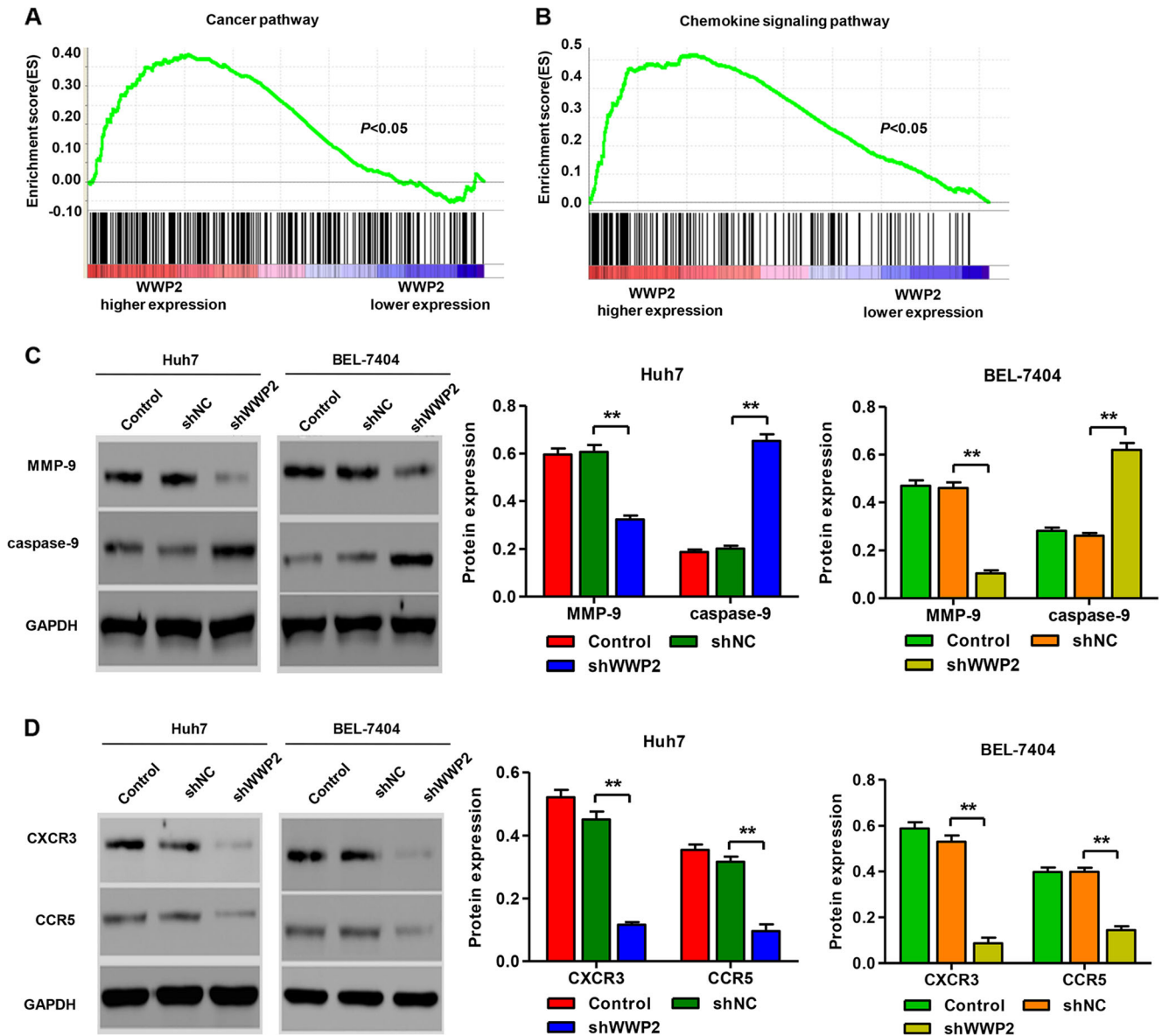
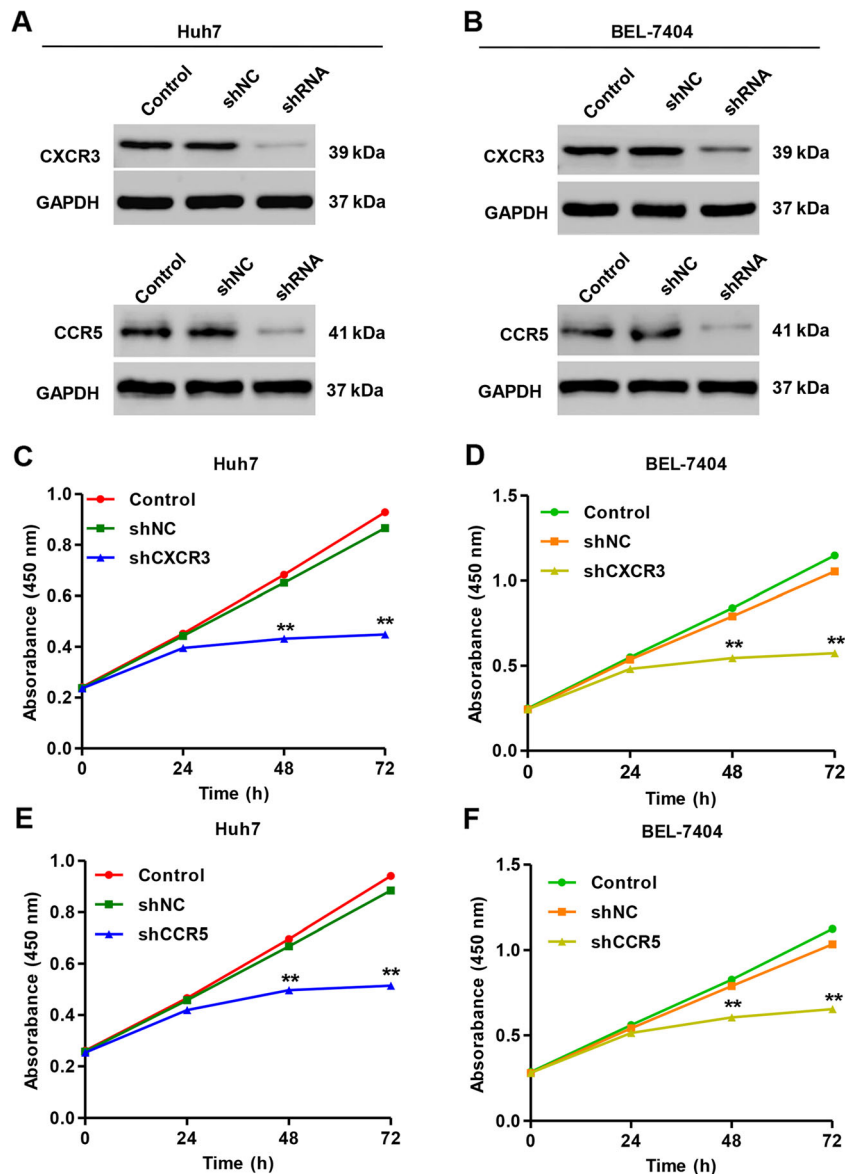


**Fig. 5** WWP2 was positively correlated to cancer pathway and the chemokine signaling pathway. Genes in the KEGG cancer pathway (a) and chemokine signaling pathway (b) showed significant enrichment in patients with higher WWP2 expression versus patients with lower WWP2 expression. The top portion of the figure plots the enrichment scores (ES) for each gene, whereas the bottom portion of the plot shows the value of the ranking metric moving down the list of ranked genes. After treatment

of Huh7 and BEL-7404 cells with shWWP2, the expression of MMP-9, caspase-9 (c), CXCR3, and CCR5 (d) were analyzed by Western blot using anti-MMP-9, anti-caspase-9, anti-CXCR3, and anti-CCR5 antibodies, as described in “Materials and methods.” Shown are representative blots of three independent studies. Means±SD are shown. \*\**P*<0.01 compared with the shNC group

**Fig. 6** The effect of CXCR3 and CCR5 on cell proliferation. After treatment of Huh7 (a) and BEL-7404 (b) cells with shCXCR3 and shCCR5, respectively, the expression of CXCR3 and CCR5 was analyzed by Western blot, as described in “Materials and methods.” Shown are representative blots of three independent studies. After treatment of Huh7 (c, e) and BEL-7404 (d, f) cells with shCXCR3 and shCCR5, respectively, cell proliferation was performed, as described in “Materials and methods.” Means±SD are shown. \*\* $P < 0.01$  compared with the shNC group



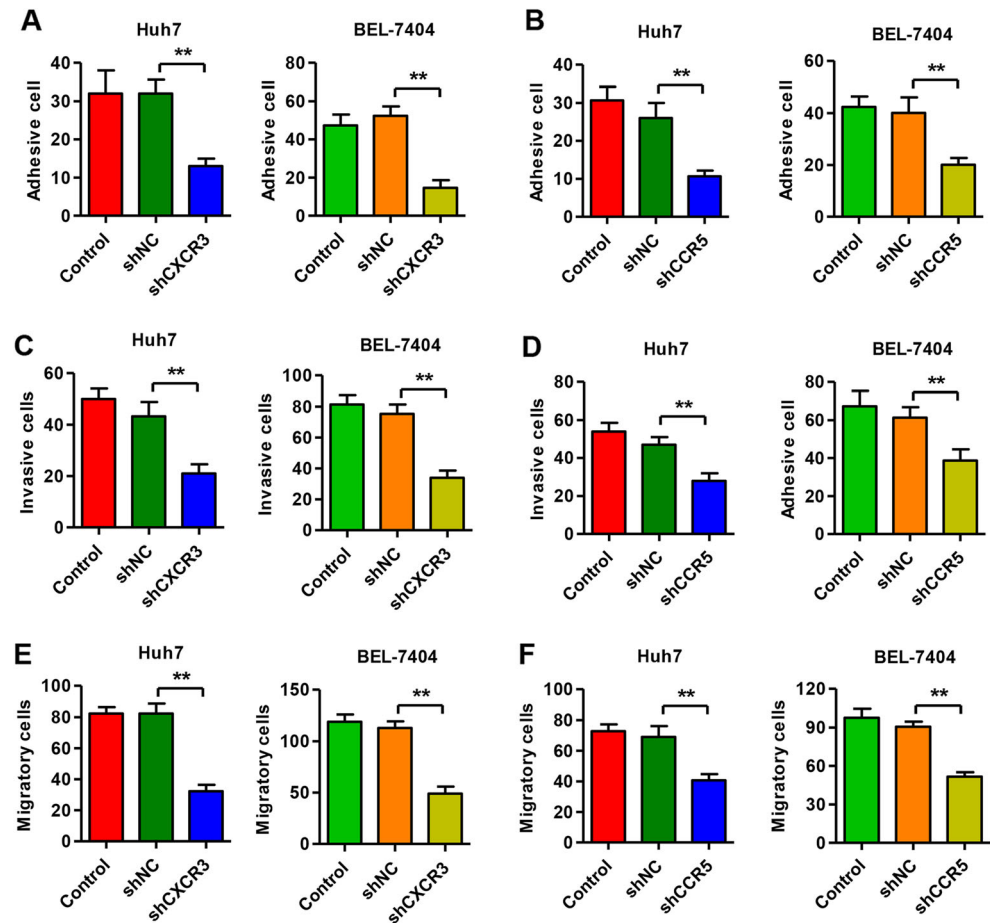
Moreover, we also found that WWP2 was positively correlated to chemokine signaling pathway and regulating the related marker expression.

We compared WWP2 expression between liver cancer tissues and adjacent tissues in People’s Hospital of Lishui and analyzed the TCGA RNA-seq data. WWP2 expression was significantly increased in liver cancer tissues, compared with the adjacent tissues in the two individual datasets (Fig. 1a–c). Our results are consistent with previous reports that WWP2 is highly expressed in breast cancer, prostate cancer, melanoma, and human embryonic stem cells [9, 31, 32]. Of note, because of the spread of intrahepatic metastasis, the highly recurrent rate plagues the long-term survival of HCC patients after curative resection [33]. In this study, the higher

WWP2 expression in liver cancer was associated with a poor prognosis in GSE20140 dataset (Fig. 1d). These results indicate that WWP2 may play important roles and can represent a new prognostic factor in liver cancer patients.

In this study, we also assessed WWP2 expression in liver cancer cell lines and found that Huh7 and BEL-7404 cell lines highly expressed WWP2 mRNA and protein (Fig. 2a, b). Moreover, silencing of WWP2 conferred a significant reduction on cell proliferation and increase in cell apoptosis in Huh7 and BEL-7404 liver cancer cell lines (Fig. 3). Invasion and migration are two of the most important marks of cancer and function as the lethal factors for malignant cancer in general and HCC in particular [34–36]. Management of migration

**Fig. 7** The effect of CXCR3 and CCR5 on cell adhesion, invasion, and migration. After treatment of Huh7 and BEL-7404 cells with shCXCR3 and shCCR5, respectively, cell adhesion (a, b), invasion (c, d), and migration (e, f) were performed, as described in “Materials and methods.” Means  $\pm$ SD are shown.  $**P < 0.01$  compared with the shNC group

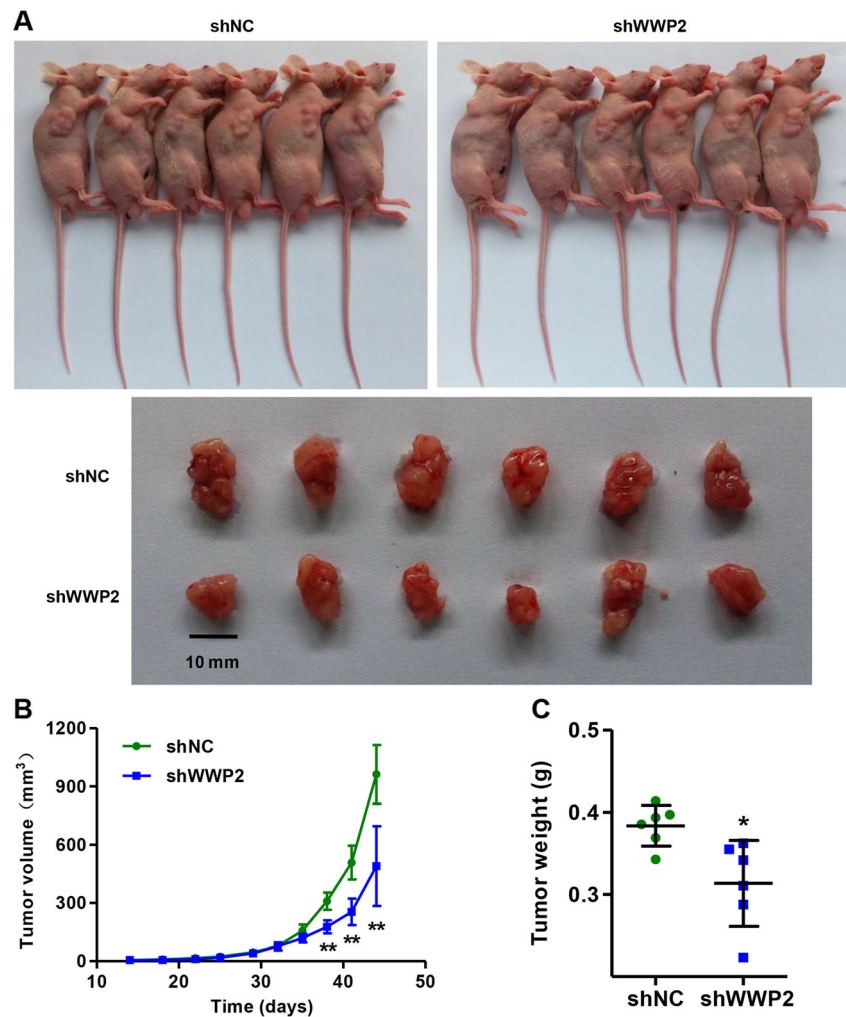


will therefore contribute to the improvement of prognosis for the HCC patient. In cultured Huh7 and BEL-7404 cells, where WWP2 was markedly expressed, silencing of WWP2 significantly inhibited cell adhesion, invasion, and migration activities compared with the shNC groups (Fig. 4). The strong correlation between WWP2 expression and liver cancer cell adhesion, invasion, and migration highlights the potential value of WWP2 as a novel biomarker for liver progression.

Despite improvement in determining the molecular mechanisms of liver cancer tumorigenesis, the specific signal transduction pathways involved have not been fully characterized. Besides, preceding evidence proves that chemokine receptor signaling also contributes to proliferation and survival, which is particularly important for migratory cells to grow in foreign environments [37, 38]. GSEA results demonstrated that cancer pathway especially the chemokine signaling pathway was significantly enriched in response to WWP2 alteration in liver cancer patients (Fig. 5a, b). Western blot analysis was consistent with that of GSEA results, in which WWP2 regulated the expression of cancer pathway- and chemokine signaling pathway-related markers, including MMP-9, caspase-9, CXCR3, and

CCR5, in Huh7 and BEL-7404 cells (Fig. 5c, d). These data suggest that silenced WWP2 inhibited liver cancer progression maybe through downregulating CXCR3 and CCR5. To examine the hypothesis, CXCR3 and CCR5 were silenced by injection of shCXCR3 and shCCR5 in Huh7 and BEL-7404 cells. Our results showed that silencing of CXCR3 and CCR5 notably reduced cell proliferation, adhesion, invasion, and migration in Huh7 and BEL-7404 cells (Fig. 6c–f and 7c–f). CXCR3 is a chemokine receptor activated by specific binding of ligands, resulting in diverse cellular responses, including cell proliferation and migration [39]. Silencing of CXCR3 conferred a migratory inhibition in breast cancer and spontaneous lung metastasis from mammary gland-implanted tumors in a murine model [40]. Interestingly, CXCR3 overexpression did not show a reduction of cell invasion and migration in PLC $\beta$ 3 knockdown DU-145 cells, suggesting that PLC $\beta$ 3 was involved in CXCR3-induced invasive and migratory inhibition [41]. Chemokine CCL5 and its receptor CCR5 were found to have increased expression in breast cancer and displayed increased invasiveness, which was blocked by CCR5 antagonists, maraviroc and vicriviroc [42].

**Fig. 8** WWP2 regulated tumor growth in vivo. **a** Xenograft tumor from nude mice was injected with Huh7 cells stably expressing shWWP2 or negative control (shNC) as described in “Materials and methods.” **b** Growth curve of tumor volumes. **c** Tumor weights. Means±SD are shown. The *asterisk* in **b** refers to 38, 41, and 44 days, respectively. \* $P < 0.05$ , \*\* $P < 0.01$  compared with the shNC group



The tumorigenic potential of WWP2 was supported by our xenograft experiments in vivo. Nude mice injected with WWP2 shRNA lentivirus stably infected (shWWP2) Huh7 cells showed tumor growth reduction when compared with the cells injected with shNC over a 45-day time period (Fig. 8). Consistent with our results, nude mice injected with WWP2 shRNA-expressing human prostate cancer DU145 cells also showed tumor growth reduction when compared with control [10]. Collectively, these results indicate the first demonstration of its crucial function in liver cancer development.

In this study, we demonstrate that WWP2 promotes cell adhesion, invasion, and migration in liver cancer by upregulating CXCR3 and CCR5 expression associated with the chemokine signaling pathway. However, further in vivo studies are needed to clarify the mechanisms of promotion of WWP2 in liver cancer tumorigenesis. WWP2 and related molecules may serve as a potential therapeutic target for metastatic liver cancer cell.

**Acknowledgments** This study was supported by the Project of science and technology of Zhejiang Province public welfare (2014c3316).

**Compliance with ethical standards**

**Conflicts of interest** None

## References

- Okuda K. Hepatocellular carcinoma. *J Hepatol.* 2000;32:225–37.
- del Pozo AC, López P. Management of hepatocellular carcinoma. *Clin Liver Dis.* 2007;11:305–21.
- Kudo M, Okanoue T. Management of hepatocellular carcinoma in Japan: consensus-based clinical practice manual proposed by the Japan Society of Hepatology. *Oncology.* 2007;72:2–15.
- Nakakura EK, Choti MA. Management of hepatocellular carcinoma. *Oncol Huntingt.* 2000;14:1085–97.
- Huang S, He X. The role of microRNAs in liver cancer progression. *Br J Cancer.* 2010;104:235–40.

6. Aravalli RN, Steer CJ, Cressman EN. Molecular mechanisms of hepatocellular carcinoma. *Hepatology*. 2008;48:2047–63.
7. Qian YW, Chen Y, Yang W, Fu J, Cao J, Ren YB, et al. P28(GANK) prevents degradation of Oct4 and promotes expansion of tumor-initiating cells in hepatocarcinogenesis. *Gastroenterology*. 2012;142:1547. e1514–58. e1514.
8. Pirozzi G, McConnell SJ, Uveges AJ, Carter JM, Sparks AB, Kay BK, et al. Identification of novel human WW domain-containing proteins by cloning of ligand targets. *J Biol Chem*. 1997;272:14611–6.
9. Xu H, Wang W, Li C, Yu H, Yang A, Wang B, et al. WWP2 promotes degradation of transcription factor OCT4 in human embryonic stem cells. *Cell Res*. 2009;19:561–73.
10. Maddika S, Kavela S, Rani N, Palicharla VR, Pokorny JL, Sarkaria JN, et al. WWP2 is an E3 ubiquitin ligase for PTEN. *Nat Cell Biol*. 2011;13:728–33.
11. Chantray A. WWP2 ubiquitin ligase and its isoforms: new biological insight and promising disease targets. *Cell Cycle*. 2011;10:2437–9.
12. Yang Y, Liao B, Wang S, Yan B, Jin Y, Shu H-B, et al. E3 ligase WWP2 negatively regulates TLR3-mediated innate immune response by targeting TRIF for ubiquitination and degradation. *Proc Natl Acad Sci*. 2013;110:5115–20.
13. Fukumoto C, Nakashima D, Kasamatsu A, Unozawa M, Shida-Sakazume T, Higo M, et al. WWP2 is overexpressed in human oral cancer, determining tumor size and poor prognosis in patients: downregulation of WWP2 inhibits the AKT signaling and tumor growth in mice. *Oncoscience*. 2014;1:807.
14. Zou W, Chen X, Shim J-H, Huang Z, Brady N, Hu D, et al. The E3 ubiquitin ligase WWP2 regulates craniofacial development through mono-ubiquitylation of gooseoid. *Nat Cell Biol*. 2011;13:59–65.
15. Nakamura Y, Yamamoto K, He X, Otsuki B, Kim Y, Murao H, et al. WWP2 is essential for palatogenesis mediated by the interaction between Sox9 and mediator subunit 25. *Nat Commun*. 2011;2:251.
16. O'Hayre M, Salanga C, Handel T, Allen S. Chemokines and cancer: migration, intracellular signalling and intercellular communication in the microenvironment. *Biochem J*. 2008;409:635–49.
17. Lazennec G, Richmond A. Chemokines and chemokine receptors: new insights into cancer-related inflammation. *Trends Mol Med*. 2010;16:133–44.
18. Rollins BJ. Inflammatory chemokines in cancer growth and progression. *Eur J Cancer*. 2006;42:760–7.
19. Yu T, Wu Y, Helman JI, Wen Y, Wang C, Li L. CXCR4 promotes oral squamous cell carcinoma migration and invasion through inducing expression of MMP-9 and MMP-13 via the ERK signaling pathway. *Mol Cancer Res*. 2011;9:161–72.
20. Lai K-C, Huang A-C, Hsu S-C, Kuo C-L, Yang J-S, Wu S-H, et al. Benzyl isothiocyanate (BITC) inhibits migration and invasion of human colon cancer HT29 cells by inhibiting matrix metalloproteinase-2/-9 and urokinase plasminogen (uPA) through PKC and MAPK signaling pathway. *J Agric Food Chem*. 2010;58:2935–42.
21. Srinivas G, Anto RJ, Srinivas P, Vidhyalakshmi S, Senan VP, Karunakaran D. Emodin induces apoptosis of human cervical cancer cells through poly (ADP-ribose) polymerase cleavage and activation of caspase-9. *Eur J Pharmacol*. 2003;473:117–25.
22. de Lemos C, Christensen JE, Nansen A, Moos T, Lu B, Gerard C, et al. Opposing effects of CXCR3 and CCR5 deficiency on CD8+ T cell-mediated inflammation in the central nervous system of virus-infected mice. *J Immunol*. 2005;175:1767–75.
23. Subramanian A, Kuehn H, Gould J, Tamayo P, Mesirov JP. GSEA-P: a desktop application for gene set enrichment analysis. *Bioinformatics*. 2007;23:3251–3.
24. Hu Y, Chen H-Y, Yu C-Y, Xu J, Wang J-L, Qian J, et al. A long non-coding RNA signature to improve prognosis prediction of colorectal cancer. *Oncotarget*. 2014;5:2230.
25. Xiong S, Zheng Y, Jiang P, Liu R, Liu X, Chu Y. MicroRNA-7 inhibits the growth of human non-small cell lung cancer A549 cells through targeting BCL-2. *Int J Biol Sci*. 2011;7:805.
26. Payton JE, Grieselhuber NR, Chang L-W, Murakami M, Geiss GK, Link DC, et al. High throughput digital quantification of mRNA abundance in primary human acute myeloid leukemia samples. *J Clin Invest*. 2009;119:1714–26.
27. Chen H-W, Yu S-L, Chen JJ, Li H-N, Lin Y-C, Yao P-L, et al. Anti-invasive gene expression profile of curcumin in lung adenocarcinoma based on a high throughput microarray analysis. *Mol Pharmacol*. 2004;65:99–110.
28. Tomayko MM, Reynolds CP. Determination of subcutaneous tumor size in athymic (nude) mice. *Cancer Chemother Pharmacol*. 1989;24:148–54.
29. Xu M, Qian G, Xie F, Shi C, Yan L, Yu L, et al. Expression of epithelial cell adhesion molecule associated with elevated ductular reactions in hepatocellular carcinoma. *Clin Res Hepatol Gastroenterol*. 2014;38:699–705.
30. Yamada S, Utsunomiya T, Morine Y, Imura S, Ikemoto T, Arakawa Y, et al. Expressions of hypoxia-inducible factor-1 and epithelial cell adhesion molecule are linked with aggressive local recurrence of hepatocellular carcinoma after radiofrequency ablation therapy. *Ann Surg Oncol*. 2014;21 Suppl 3:S436–42.
31. Soond SM, Smith PG, Wahl L, Swingler TE, Clark IM, Hemmings AM, et al. Novel WWP2 ubiquitin ligase isoforms as potential prognostic markers and molecular targets in cancer. *Biochim Biophys Acta (BBA) Mol Basis Dis*. 2013;1832:2127–35.
32. Nguyen Huu NS, Ryder WDJ, Zeps N, Flaszka M, Chiu M, Hanby A, et al. Tumour-promoting activity of altered WWP1 expression in breast cancer and its utility as a prognostic indicator. *J Pathol*. 2008;216:93–102.
33. Matsuo N, Shiraha H, Fujikawa T, Takaoka N, Ueda N, Tanaka S, et al. Twist expression promotes migration and invasion in hepatocellular carcinoma. *BMC Cancer*. 2009;9:240.
34. Fransvea E, Angelotti U, Antonaci S, Giannelli G. Blocking transforming growth factor-beta up-regulates E-cadherin and reduces migration and invasion of hepatocellular carcinoma cells. *Hepatology*. 2008;47:1557–66.
35. Li N, Fu H, Tie Y, Hu Z, Kong W, Wu Y, et al. miR-34a inhibits migration and invasion by down-regulation of c-Met expression in human hepatocellular carcinoma cells. *Cancer Lett*. 2009;275:44–53.
36. Burk U, Schubert J, Wellner U, Schmalhofer O, Vincan E, Spaderna S, et al. A reciprocal repression between ZEB1 and members of the miR-200 family promotes EMT and invasion in cancer cells. *EMBO Rep*. 2008;9:582–9.
37. Sugiyama T, Kohara H, Noda M, Nagasawa T. Maintenance of the hematopoietic stem cell pool by CXCL12-CXCR4 chemokine signaling in bone marrow stromal cell niches. *Immunity*. 2006;25:977–88.
38. Mantovani A, Allavena P, Sica A, Balkwill F. Cancer-related inflammation. *Nature*. 2008;454:436–44.
39. Dagan-Berger M, Feniger-Barish R, Avniel S, Wald H, Galun E, Grabovsky V, et al. Role of CXCR3 carboxyl terminus and third intracellular loop in receptor-mediated migration, adhesion and internalization in response to CXCL11. *Blood*. 2006;107:3821–31.
40. Ma X, Norsworthy K, Kundu N, Rodgers WH, Gimotty PA, Golubeva O, et al. CXCR3 expression is associated with poor survival in breast cancer and promotes metastasis in a murine model. *Mol Cancer Ther*. 2009;8:490–8.
41. Wu Q, Dhir R, Wells A. Altered CXCR3 isoform expression regulates prostate cancer cell migration and invasion. *Mol Cancer*. 2012;11.
42. Velasco-Velázquez M, Jiao X, De La Fuente M, Pestell TG, Ertel A, Lisanti MP, et al. CCR5 antagonist blocks metastasis of basal breast cancer cells. *Cancer Res*. 2012;72:3839–50.